Evaluation of the Mitral and Aortic Valves With Cardiac CT Angiography

Samir V. Chheda, BS, Monvadi B. Srichai, MD, Robert Donnino, MD, Danny C. Kim, MD, Ruth P. Lim, MBBS, and Jill E. Jacobs, MD

Abstract: Cardiac computed tomographic angiography (CTA) using multidetector computed tomographic scanners has proven to be a reliable technique to image the coronary vessels. CTA also provides excellent visualization of the mitral and aortic valves, and yields useful information regarding valve anatomy and function. Accordingly, an assessment of the valves should be performed whenever possible during CTA interpretation. In this paper, we highlight the imaging features of common functional and structural left-sided valvular disorders that can be seen on CTA examinations.

Key Words: computed tomography, cardiac, valves, angiography

(*J Thorac Imaging* 2010;25:76–85)

Cardiac computed tomographic angiography (CTA) obtained on multidetector computed tomographic (MDCT) scanners is routinely used to evaluate the coronary arteries. In addition to enabling assessment of the heart vessels, the contrast opacification of the cardiac chambers provides excellent visualization of the mitral and aortic valves.

In this pictorial essay, we review the normal imaging appearance of the mitral and aortic valves on CTA. In addition, we discuss and illustrate CTA features of functional valve disease [mitral stenosis (MS), mitral regurgitation (MR), aortic stenosis (AS), and aortic insufficiency (AI)] and structural valve abnormalities [mitral valve prolapse (MVP), endocarditis, valvular tumors, thrombi, and prosthetic heart valves]. Finally, we discuss the relative strengths and limitations of CTA in assessing valve disease relative to echocardiography and cardiac magnetic resonance imaging (MRI).

NORMAL VALVE STRUCTURE AND FUNCTION

Mitral Valve

The mitral valve apparatus is composed of 5 parts: an annulus, 2 leaflets, 2 commissures, 2 papillary muscles, and chordae tendinae (Figs. 1, 2). Appropriate function of the valve requires synchronous action between all components.

The annulus is a saddle-shaped fibrous ring embedded in the myocardium of the morphologic left ventricle. It functions as an anchor for the mitral valve leaflets. The annulus shares structural continuity with the aortic annulus through 3 fibrous trigones (Fig. 1). Owing to this anatomic connection, diseases of the mitral annulus can affect the aortic annulus and vice versa.[1] Unless the mitral annulus is calcified, its border is difficult to identify on CTA.[2]

The mitral valve is the only cardiac valve with 2 leaflets. The anterior leaflet is semicircular in shape, whereas the posterior leaflet is rectangular. Owing to its position within the left ventricle, the anterior leaflet also functions as a separation between the inflow and outflow tracts of the left ventricle.

The 2 commissures are clefts that divide the 2 leaflets from each other. In some pathologic states, however, the commissural spaces may become obliterated and the leaflets appear fused.

The papillary-chordal apparatus connects the mitral leaflets to the left ventricle. The 2 papillary muscles (anterolateral and posteromedial) arise from the free (lateral) wall of the left ventricle and can usually be seen on long-axis views of the heart (Figs. 1, 3). The 3-chamber view is particularly useful for observing the posteromedial muscle (Fig. 1).[2] The chordae tendinae are fibrous tendons which arise from each papillary muscle and insert on the free edge of both leaflets (Fig. 1). Each leaflet receives chordae from each of the 2 papillary muscles.[1]
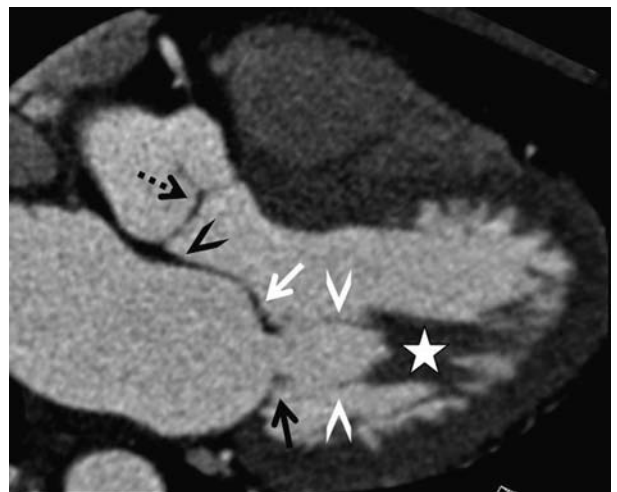

FIGURE 1. Three-chamber MPR image shows the anterior mitral leaflet (white arrow), the posterior mitral leaflet (black arrow), posteromedial papillary muscle (white star), and corresponding chordae tendinae (white arrowheads). Note the structural continuity (black arrowhead) between the mitral and aortic valves (dotted arrow). MPR indicates multiplanar reformation.

From the Department of Radiology, New York University Langone Medical Center, New York, NY.
Reprints: Jill E. Jacobs, MD, Department of Radiology, New York University Langone Medical Center, 560 First Avenue, New York, NY 10016 (e-mail: jill.jacobs@nyumc.org).

FIGURE 2. Short-axis MPR images through the mitral valve show the anterior leaflet (arrow) and posterior leaflet (arrowhead) in diastole (A) and systole (B). In systole, note the invagination and overlap of the closed leaflets. Three-chamber MPR image of the mitral valve in systole (C) also shows the overlap (white arrow) of the mitral leaflets. MPR indicates multiplanar reformation.

During systole, the papillary muscles contract, tensing the chordae and pulling the leaflets together until they coapt (Fig. 3B). As the chordae insert on the free edge of the leaflets, the true closing edge of the leaflets is slightly proximal to the free edge, resulting in an overlap of the leaflets in systole (Figs. 2B, C). During diastole, as the pressure in the left ventricle decreases, the mitral leaflets open into the left ventricle (Fig. 3A).

Aortic Valve

The aortic valve is composed of an annulus, 3 cusps, and 3 commissures. As in the mitral valve, the aortic annulus is a fibrous ring embedded in the endocardium at the sinotubular junction to which the 3 cusps attach. Unlike the mitral valve, the aortic valve lacks chordae tendinae and papillary muscles.

The 3 aortic cusps (right, left, and posterior) are "half-mooned" in shape; hence, the aortic valve is commonly referred to as a semilunar valve (Fig. 4). In the closed position, each cusp forms a pocket that opens into the ascending aorta. Behind each cusp is a dilation of the aorta known as the sinus of Valsalva (Fig. 5). The right and left coronary arteries arise from the sinuses of the right and left cusps, respectively. The posterior cusp lacks a corresponding coronary artery; hence, its name, the noncoronary cusp. Separating the 3 aortic cusps are the 3 aortic commissures, which are roughly equally spaced around the valve annulus (Fig. 4).

In systole, the pressure in the left ventricle exceeds that of the aorta, causing the aortic cusps to open (Figs. 4B, 5B).

In this position, the cusps produce a triangular-shaped orifice that molds to the circular structure of the annulus.[1] In diastole, as the left ventricular pressure declines, the aortic cusps coapt against each other (Figs. 4A, 5A). As in the case of the mitral leaflets, the closing edge of the aortic cusps is slightly proximal to the true free edge of each cusp, creating an area of overlap between the surfaces of the 3 cusps.

MITRAL STENOSIS

MS is defined as a narrowing of the mitral valve orifice to less than 2.5 cm^2.[3] Using a planimetry technique, one can directly measure the area of the mitral valve orifice on CTA (Table 1).[4] To perform planimetry, one must determine the phase in early-to-mid diastole when the mitral valve is maximally open. This is accomplished using 4-chamber and 2-chamber views of the heart, with the long axis on the 2-chamber view positioned from the center of the valve to the left ventricular apex. A short-axis view of the mitral valve at the tips of the leaflets is then obtained perpendicular to the long-axis planes. Using a planimetry tool, the valve orifice is traced on the short-axis view and the valve area is calculated.

Secondary signs of MS on CTA include left atrial enlargement with an anatomically normal left ventricle (Fig. 6B). Very chronic and severe MS commonly results in pulmonary vein dilation, pulmonary venous hypertension, and right ventricular hypertrophy.[5]

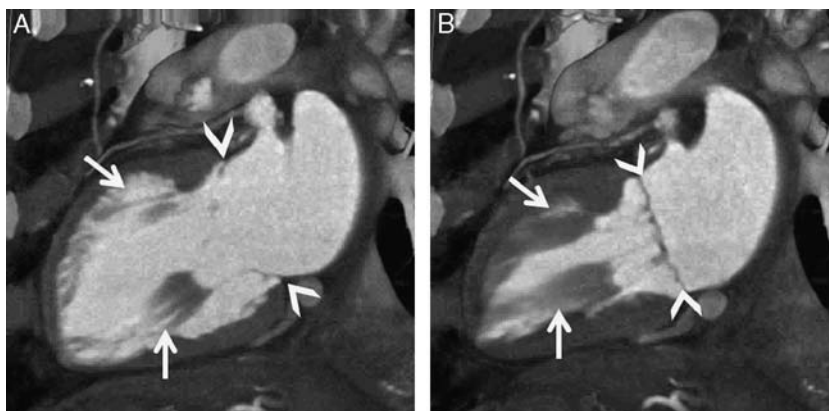Most cases of MS are caused by rheumatic heart disease, and rheumatic pathology is found in 99% of

FIGURE 3. Two-chamber multiplanar reformation images of the mitral valve. In diastole (A), the papillary muscles (arrows) are relaxed, and the leaflets (arrowheads) completely open. In systole (B), the papillary muscles contract and the leaflets coapt.
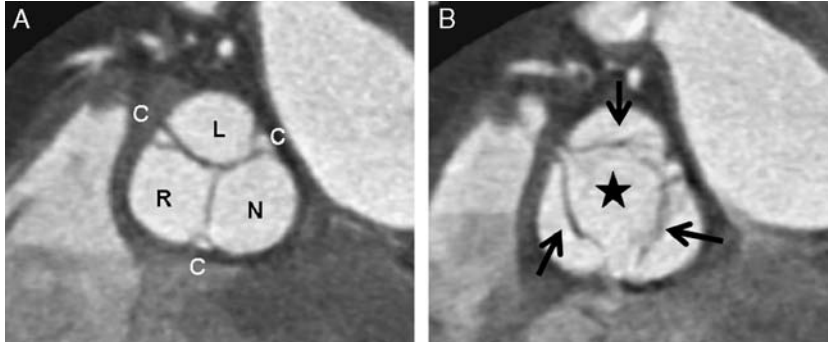
FIGURE 4. Short-axis multiplanar images through the aortic valve. The aortic valve is composed of 3 cusps left (L), right (R), and noncoronary (N), and 3 commissures (C). In diastole (A), the 3 cusps firmly oppose each other, sealing off the ascending aorta. In systole (B), the cusps (black arrows) fold into the walls of the aorta, creating a rounded, triangular-shaped orifice (black star).

surgically replaced stenotic mitral valves.[6] Other rare causes of MS include congenital stenosis, degenerative calcification, radiation fibrosis, and endocarditis.[5]

The CTA features of rheumatic MS include thickening and calcification of the valve leaflets and/or annulus; fusion of the commissures; and thickening, shortening, and calcification of the chordae (Fig. 6).[6] In rheumatic MS, the leaflet tips are commonly affected first. Consequently, the leaflets may become "dome shaped," as the bases of the leaflets remain mobile whereas the tips are restricted in motion (Fig. 6B). As the disease progresses, the entire leaflets may immobilize. In very severe disease, the leaflets may become so rigid and adherent to each other that they can neither open nor shut.[6]

MITRAL REGURGITATION

MR is the backflow of blood from the left ventricle to the left atrium resulting from incomplete closure of the mitral valve. The main imaging feature of MR on CTA is incomplete coaptation of the valve leaflets in systole (Fig. 7), resulting in a regurgitant orifice. The regurgitant orifice area can be measured on CTA using a planimetry technique (Table 1).[7]

The causes of MR can be divided into disease of the valve leaflets or their supporting structures. Primary leaflet disorders include MVP, rheumatic heart disease, endocarditis, collagen vascular disease, and certain serotonergic drugs that cause cardiac fibrosis, for example, fenfluramine. Causes of MR secondary to disease of the leaflets' supporting structures include ruptured chordae tendinae, ruptured papillary muscles, and papillary muscle dysfunction without rupture. In addition, hypertrophic cardiomyopathy with systolic anterior motion of the anterior leaflet, dilated cardiomyopathy with displacement of the papillary muscles, and ischemic heart disease with apical tethering of the leaflets, chordae tendinae, and/or papillary muscles can result in secondary MR. Although MR is usually a chronic disease, it may present abruptly as in the case of ruptured chordae tendinae or endocarditis.[3,8]

Depending on the etiology, other pathologic features associated with MR that can be seen on CTA include annulus and/or leaflet calcification; annulus dilation; leaflet thickening (Fig. 7) and prolapse; shortened or elongated chordae; hypokinetic papillary muscles; and mixed MS/MR. Ruptured chordae tendinae is an uncommon etiology of MR that can be difficult to observe on CTA.[7] In chronic cases of severe MR, the left ventricle and left atrium will

FIGURE 5. Three-chamber multiplanar images of the aortic valve. In diastole (A), the cusps' coaptation leads to some overlap (black arrow). In systole (B), the cusps (white arrows) fold into the walls of the aorta. Also, note the dilations of the aorta known as the sinuses of Valsalva (black arrowheads).

TABLE 1. Valve Areas in Left-sided Valve Disease Based on Echocardiographic Standards[3]*

	Normal Mitral Valve Area	Mild Disease	Moderate Disease	Severe Disease
Mitral stenosis				
Valve area (cm^2)	4.0-5.0	1.5-2.5	1.0-1.5	< 1.0
Mitral regurgitation				
Regurgitant orifice area (cm^2)		< 0.20 cm	0.20-0.39	≤0.40
Aortic stenosis				
Valve area (cm^2)	3.0-4.0	1.5-3.0	1.0-1.5	< 1.0
Aortic insufficiency				
Regurgitant orifice area (cm^2)		< 0.10 cm	0.10-0.29	≤0.30

*Standard measurements from computed tomographic angiography have yet to be established.

typically be dilated, but in acute MR, marked interstitial pulmonary edema may be seen whereas the chambers' sizes remain relatively normal.[9]

AORTIC STENOSIS

Valvular aortic stenosis is the obstruction of blood flow across the aortic valve caused by valve narrowing. CTA has been validated as an excellent technique to visualize and measure the aortic valve orifice area by planimetry (Table 1).[10–13]

The main etiologies of aortic valvular stenosis include congenital bicuspid aortic valves, age-related calcification of an anatomically normal valve, and rheumatic valve disease.[6] In the United States, among patients under the age of 65 years who present with AS, congenital bicuspid aortic valve is the most common etiology.[8] This anomaly occurs in 1% to 2% of the general US population.[8] In the majority of patients born with bicuspid aortic valves, stenosis is not congenital, but results exclusively from subsequent calcification of the abnormal valve. Congenital bicuspid valves consist of 2 unequally sized aortic cusps (Fig. 8). The cusps can either be oriented in an anterior-posterior or in left-right direction. In some cases, a midline raphe down

one of the valve cusps is present, denoting the area where a failed division of the third cusp occurred.[14] In addition to AS, congenital bicuspid aortic valves may present with combined AS/AI, isolated AI, or no functional valve disease. Rare congenital anomalies that can also present with AS include unicuspid, indeterminate, and hypoplastic aortic valves.[6] Quadricuspid valves, another rare malformation, usually present with AI.[15] Among patients over the age of 65 years who present with AS in the United States, age-related calcification of an anatomically tricuspid valve is the most common etiology (Fig. 9).[8] The pathologic process is hypothesized to be similar to the disease process of atherosclerosis. Although rheumatic heart disease is the most common worldwide cause of AS, it is uncommon in the United States. In patients with rheumatic AS (Fig. 10), there is a 95% concomitance with rheumatic mitral valve disease.[3]

On CTA, structural features of the aortic valve can aid in determining the etiology of AS. Although cusp thickening is a similar feature throughout each of the etiologies of AS, the pattern of calcification varies significantly. In age-related AS, the calcification usually begins at the valve annulus and progresses throughout the cusps; this calcification is often very heavy and asymmetric, leading to an
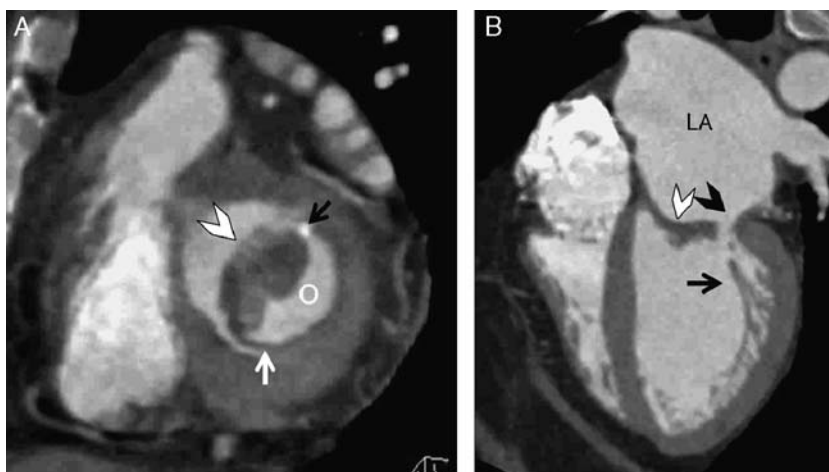
FIGURE 6. Rheumatic MS. Short-axis MPR image through the mitral valve in diastole (A) and 4-chamber MPR images in diastole (B) show a severely thickened anterior leaflet (white arrowheads) that is unable to retract, leading to a stenotic orifice (O in ''A'' and black arrowhead in ''B''). The leaflet tip is more thickened than the leaflet base, causing a ''doming'' of the leaflet (white arrowhead in ''B''). The posterior leaflet is not significantly affected and is able to completely retract (white arrow). In addition, there is calcification of the commissures (black arrow in ''A''), fusing the 2 leaflets. The papillary-chordal apparatus is also thickened and shortened (black arrow in ''B'') and the LA (left atrium) is dilated. MPR indicates multiplanar reformation.
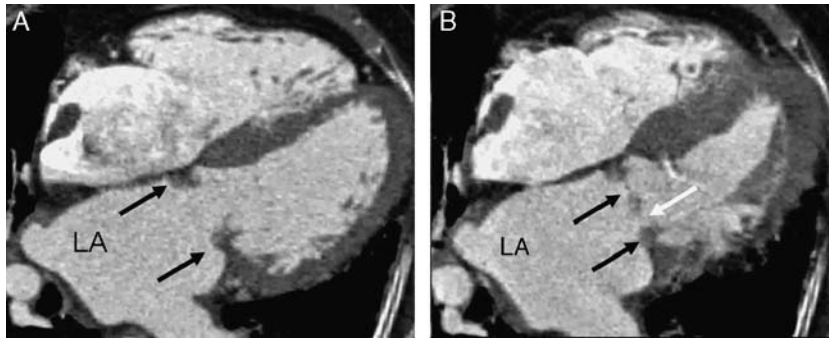
FIGURE 7. Four-chamber multiplanar images of a regurgitant mitral valve. In diastole (A), the thickened valve leaflets (black arrows) open, but in systole (B), they fail to coapt, leading to a regurgitant orifice (white arrow). Note the dilated LA (left atrium).

asymmetric opening and closing of the valves (Fig. 9). In some cases where calcification extends from 1 cusp to the next, the 2 cusps may fuse (without fusion of the commissures), resulting in a functional bicuspid valve (Fig. 11). In congenital bicuspid aortic disease, calcification is less severe and usually occurs only along the commissural edges (Fig. 8) or outlining a leaflet raphe, if one is present. Rheumatic AS typically causes symmetric calcification and fusion of the 3 commissures, resulting in a symmetric reduction in movement of the cusps (Fig. 10). Frequently, the cusps become so stiffened that they can neither fully open nor close, resulting in concomitant AS and AI.[3,9] Other imaging features of AS on CTA include concentric left ventricular hypertrophy and ascending aorta dilation.[9]

AORTIC INSUFFICIENCY

AI is the backflow of blood from the aorta to the left ventricle that results from incomplete closure of the aortic

FIGURE 8. Short-axis systolic multiplanar image of a congenital bicuspid aortic valve. The valve's 2 cusps (white arrows) do not fully retract, leading to a stenotic orifice (O). In addition, a small amount of calcification (black arrow) is present along the leaflet's commissural edge.

valve. Regardless of etiology, the common imaging feature of AI is incomplete coaptation of the valve leaflets during diastole (Figs. 10A, 12). One can use CTA to measure the regurgitant orifice area of insufficient aortic valves (Table 1).[16] Additional imaging features of AI depend on the chronicity of the disease. In chronic AI, there is an adaptive dilation of the left ventricle. If the disease is severe enough, there is also dilation of the left atrium. With acute AI, the left ventricle does not have time to adapt to the regurgitant volume, resulting in acute pulmonary congestion with a normal left ventricular size.[9]

The causes of AI are divided into diseases that affect the aortic leaflets and diseases that dilate the aortic root. Leaflet causes of AI include rheumatic heart disease, endocarditis, and bicuspid aortic valves. Causes of aortic root dilatation include hypertension, aortic aneurysm/dissection, syphilis, and vascular connective tissue disorders.[6]

MITRAL VALVE PROLAPSE

MVP is a displacement of one or both of the mitral leaflets into the left atrium during systole. By echocardiographic standards, diagnosis of MVP requires a 2 mm displacement of one or both of the mitral leaflets past the mitral annulus in a long-axis view (analogous to the 3-chamber view on CTA) of the heart.[6] The prevalence of this finding in the general population is 1% to 2.5%, and the majority of affected individuals are asymptomatic.[3]

The etiologies of MVP are divided into primary and secondary causes. In primary MVP, also known as myxomatous mitral valve, loose myxomatous tissue replaces the usually dense connective tissue of the mitral leaflet. In secondary MVP, there is an abnormality of the mitral valve leaflets in association with a systemic connective tissue disorder. Anatomically normal mitral leaflets may also prolapse when there is dysfunction of the leaflets' supporting structures, including dilation of the mitral annulus, an undersized left ventricle, and papillary muscle dysfunction.[6,8]

On CTA, MVP is characterized by displacement of one or both of the mitral leaflets into the left atrium during systole (Fig. 13). Leaflet prolapse should be assessed principally on a 3-chamber view of the heart. Owing to the saddle-shaped geometry of the mitral annulus, the leaflets can appear to prolapse on a 4-chamber view of the heart, when in reality they only rise to the plane of the annulus. Isolated posterior leaflet prolapse is most
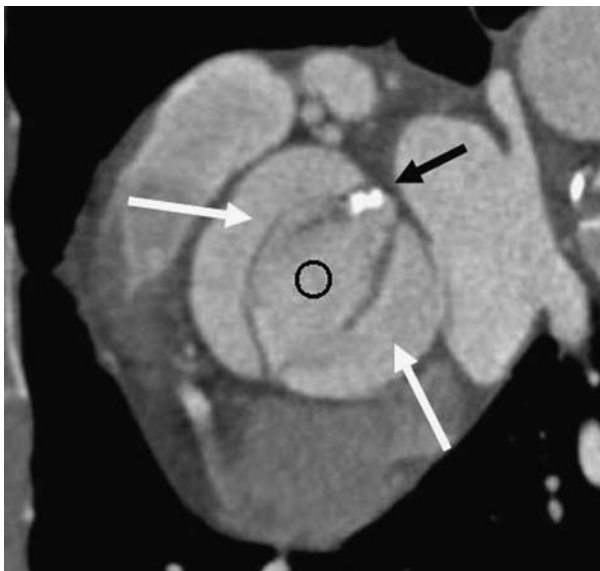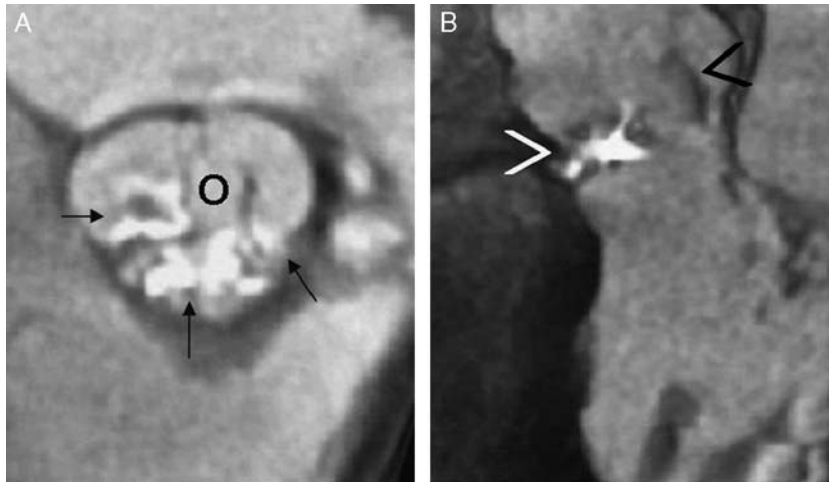
FIGURE 9. Short-axis systolic MPR image (A) of a stenotic aortic valve with age-related calcification. There is an asymmetric, heavy deposition of calcium (black arrows) on all 3 cusps, leading to impaired retraction of the cusps and a stenotic orifice (O). On the 3-chamber systolic MPR image of the valve (B), the more calcified cusps (white arrowhead) are more immobilized than the less calcified cusp (black arrowhead), leading to asymmetric opening of the valve. MPR indicates multiplanar reformation.

common, but anterior leaflet prolapse can also occur.[6] In more severe cases of primary MVP, additional CTA findings include incomplete coaptation of the mitral leaflets during systole, leaflet thickening, flail leaflet (where the prolapsed leaflet tip turns outward, becoming concave to the left atrium), and elongation of the chordae tendinae (Fig. 13).[6]

VALVULAR MASSES

Various masses can form on the mitral and aortic valves leading to functional valvular heart disease. These masses include endocarditic vegetations, fibroelastomas and other cardiac tumors, and thrombi.

Valvular Endocarditis

Infective valvular endocarditis is a rapidly progressive, life-threatening illness affecting 3.6 to 7.0 people per 1,00,000 per year.[6] Patients with other valvular diseases are at an increased risk of infection. The characteristic pathologic lesions of endocarditis are vegetations, or masses of platelets, fibrin, microorganisms, and inflammatory cells deposited on the valve leaflets. Except in the case of intravenous drug abuse, the left side of the heart is affected more frequently than the right, with mitral valve involvement more common than aortic valve involvement.[6] Vegetations typically deposit on the atrial side of the mitral valve and the ventricular side of the aortic valve.[17] In addition, valvular vegetations may form in association with noninfectious causes of endocarditis such as Libman-Sacks endocarditis in systemic lupus erythematous and Löffler endocarditis in hypereosinophilia.

On CTA, endocarditic vegetations appear as soft-tissue masses on the valve leaflets with possible secondary deformity of the valve architecture. CTA can also identify associated complications of endocarditis, including valve regurgitation, leaflet perforation, and paravalvular abscess cavities.[18]
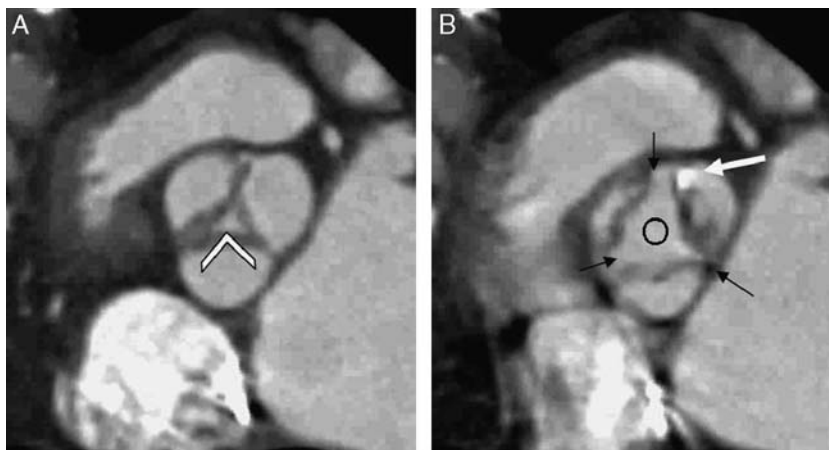

FIGURE 10. Short-axis multiplanar images of a rheumatic aortic valve. Fusion and mild calcification (white arrow) of the commissures (black arrows) results in rigid cusps, creating a regurgitant orifice (white arrowhead) in diastole (A) and a stenotic orifice (O) in systole (B).
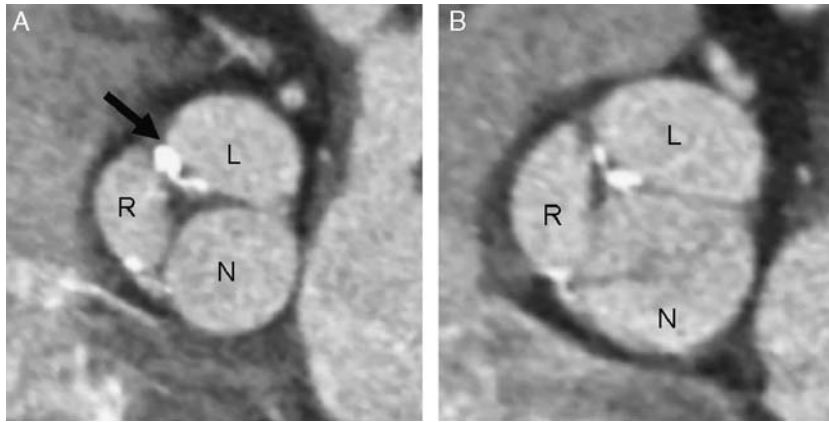
FIGURE 11. Short-axis multiplanar images of a functional bicuspid aortic valve in diastole (A) and systole (B). Calcification (black arrow) extends from the right cusp (R) to the left cusp (L), fusing the cusps into a single working unit. N indicates noncoronary cusp.

Papillary Fibroelastomas

Although rare, papillary fibroelastomas are the most common neoplasm affecting the cardiac valves.[19] Overall, these benign tumors are the second most common primary cardiac neoplasm behind myxomas.[19] Other tumors that infrequently form on the cardiac valves include myxomas and fibromas.[6] On gross pathology, papillary fibroelastomas usually consist of a 1-cm round mass emanating from
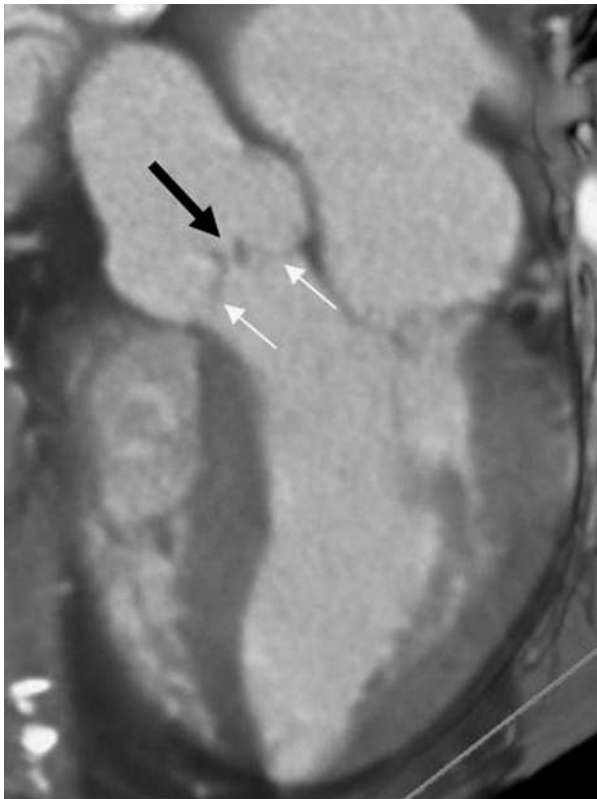

FIGURE 12. Three-chamber diastolic maximum intensity projection image of a regurgitant aortic valve of uncertain etiology. There is failed coaptation of the cusps (white arrows), leading to a regurgitant orifice (black arrow).

a 1 to 3 mm stalk with numerous papillary fronds arising from the surface.[6] In a case series of 725 patients with papillary fibroelastomas, the aortic valve was involved in 44% of the cases, and the mitral valve in 35% of the cases.[19] In the remaining patients, the tumor occurred on the tricuspid valve, the pulmonic valve, or on the endocardial surface of the cardiac chambers. Although the majority of patients are asymptomatic, complications may develop from embolization of tumor fragments or thrombi formed on the tumor surface.[6]

On CTA, papillary fibroelastomas appear as small, mobile, pedunculated valvular masses that flutter with valve motion. In addition, there is often a stippled edge outlining the mass, consistent with the tumor's papillary fronds (Fig. 14).[20]

Valvular Thrombi

Valve thrombosis is a serious condition that can result in valve dysfunction and systemic thromboembolism. Thrombus formation of the native cardiac valves is a very rare event, usually associated with intrinsic valve disease, a hypercoaguable state, or a systemic autoimmune disease.[21] More commonly, thrombus may form on mechanical prosthetic heart valves in patients not on anticoagulant therapy. Thrombus formation on bioprosthetic valves is uncommon.

On CTA, valvular thrombi appear as heterogeneous, soft-tissue density masses with irregular borders. They often obstruct and impair the normal movement of the cardiac valves.

VALVE PROSTHESIS

In addition to imaging native cardiac valve pathology, CTA can assess the structure and function of prosthetic heart valves. Currently, the most frequently implanted valve in the world is the St Jude bileaflet tilting disk valve, which consists of 2 semicircular disks that pivot between an open and closed position (Fig. 15).[6] Bioprosthetic valves (Fig. 16), for example, the Carpentier-Edwards bovine pericardial valve, are also commonly encountered in practice; these valves are derived from human or animal tissue. In general, bioprosthetic valves are less durable than mechanic valves, but pose less risk of thromboembolism.[6] In addition to total prosthetic valves, annuloplasty rings
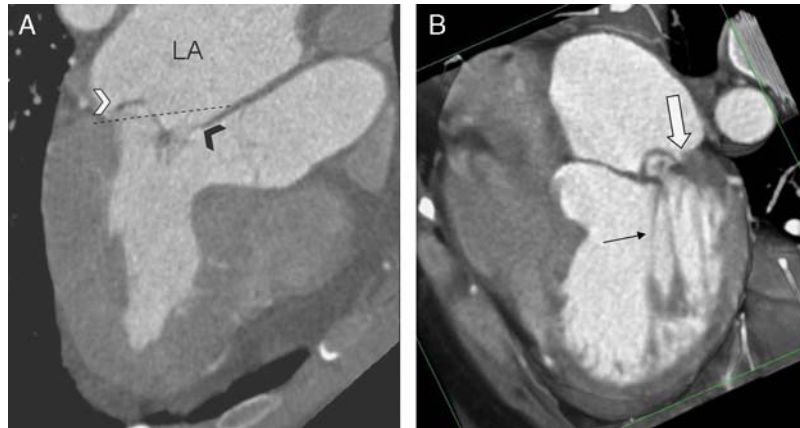
FIGURE 13. Three-chamber MPR image (A) shows a greater than 2 mm prolapse of the posterior mitral valve leaflet (white arrowhead) past the plane of the mitral annulus (broken line) into the LA (left atrium). The anterior leaflet (black arrowhead) is not affected. The 4-chamber MPR image (B) also shows thickening of the leaflet (white arrow) and elongation of the chordae tendinae (black arrow). MPR indicates multiplanar reformation. (Color figure available at www.thoracicimaging.com)

(Fig. 16) may be inserted in the mitral annulus to treat MR. These prosthetic rings reduce the annular circumference and facilitate leaflet coaptation.

A potential limitation of echocardiographic assessment of prosthetic valves is the presence of acoustic shadowing, which can impair accurate visualization of the valve prosthesis and associated pathology, including vegetations, paravalvular abscesses, and thrombi.[22] CTA usually enables assessment of prosthetic valves and their associated pathology.[18,23,24] A potential limitation of CTA is metallic streak artifact. The degree of artifact is variable depending on the imaging technique used and the type of prosthetic valve implanted (Fig. 15). Nevertheless, improvements in MDCT scanner technologies have significantly decreased this artifact.[18]

STRENGTHS AND LIMITATIONS OF CTA VERSUS OTHER IMAGING MODALITIES

Echocardiography (echo) is the most widely used imaging modality for evaluating valve disease. It is readily available, cost-effective, and very safe for the patient. As it provides all of the fundamental information that guides diagnosis and treatment of valve disease, including valve flow measurements, echo is the primary imaging modality for cardiac valve assessment. Nevertheless, echo is operator-dependent and has high interobserver variability. In addition, poor acoustic windows and a patient's body habitus can limit image quality. Acoustic shadowing, described above, also limits the evaluation of prosthetic valves.

Relative to echocardiography, cardiac MRI provides improved anatomic detail of the cardiac valves, while also allowing the quantification of valve flow and avoiding radiation and contrast risks. However, cardiac MRI is very expensive, not readily available, and requires a long acquisition time. In addition, well-documented contraindications limit MRI for certain patients.

The relatively high spatial resolution of MDCT scanners used in cardiac CTA provides a superiorly detailed depiction of valve anatomy relative to echocardiography and cardiac MRI. Accordingly, many imaging features of functional valve disease and structural valve abnormalities are best visualized on CTA. Nevertheless, the radiation and contrast risks, along with the inability to measure valve
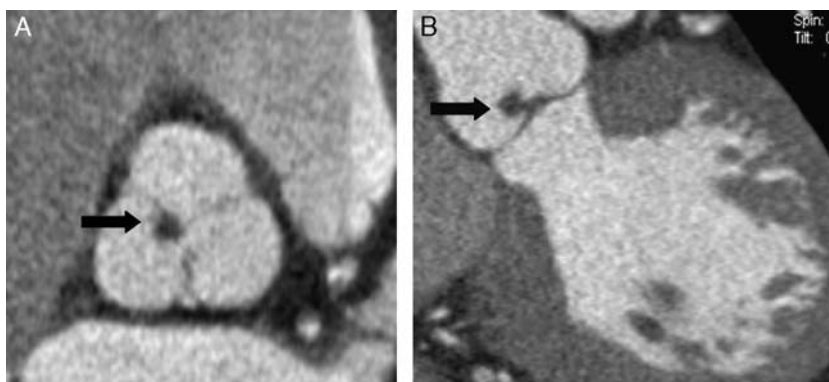

FIGURE 14. Short-axis MPR image (A) and long-axis MPR image (B) of the aortic valve show a pedunculated papillary fibroelastoma (arrow) attached to the right cusp. The diagnosis of papillary fibroelastoma was pathologically confirmed. MPR indicates multiplanar reformation.
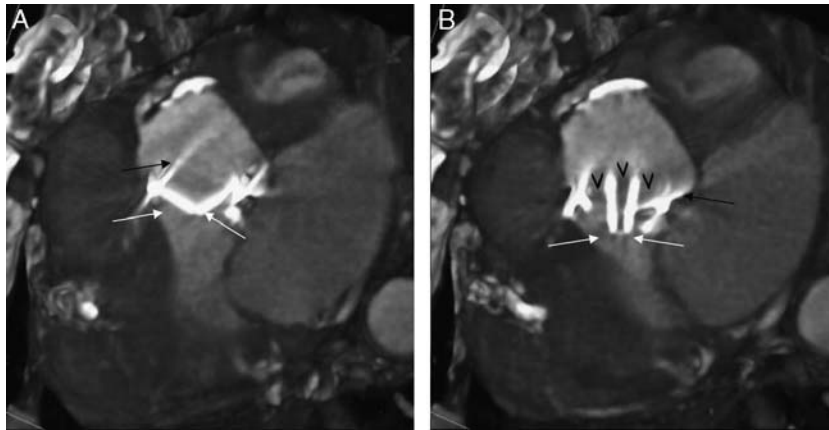
FIGURE 15. Long-axis multiplanar images of a St Jude's mechanical aortic valve. The valve consists of 2 disks (white arrows) that rotate between a closed position in diastole (A) and an open position in systole (B). The valve has 3 orifices (black arrowheads). Note the metallic streak artifacts (black arrows) around the annulus of the valve.

flow, precludes the use of cardiac CTA as a primary modality for cardiac valve assessment.

CONCLUSIONS

In addition to enabling assessment of the coronary arteries, cardiac CTA on MDCT provides valuable and detailed morphologic and functional information on the left-sided heart valves. Accordingly, the structural and functional characteristics of the valves should be assessed whenever possible on these studies.
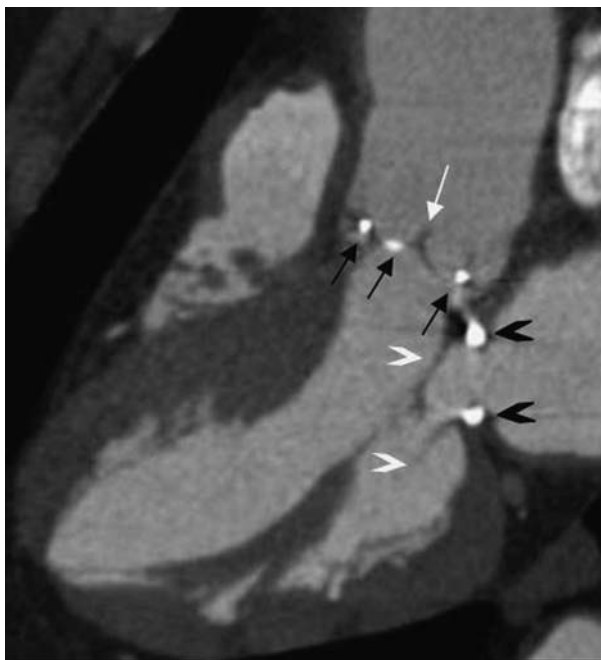

FIGURE 16. Long-axis multiplanar image of a bioprosthetic aortic valve and mitral annuloplasty ring in diastole. The aortic valve consists of a tissue prosthesis (white arrow) and metal stents (black arrows). The mitral annuloplasty ring consists of a metal ring (black arrowheads), encircling the native mitral valve (white arrowheads).

REFERENCES

1. Malouf JF, Edwards WD, Tajik AJ, et al. Functional anatomy of the heart. In: Fuster V, O'Rourke RA, Walsh RA, et al, eds. *Hurst's the Heart*. 12th ed. New York, NY: McGraw-Hill; 2008:49–82.
2. O'Brien JP, Srichai MB, Hecht EM, et al. Anatomy of the heart at multidetector CT: what the radiologist needs to know. *Radiographics*. 2007;27:1569–1582.
3. Bonow RO, Carabello BA, Chatterjee K, et al. ACC/AHA 2006 guidelines for the management of patients with valvular heart disease: a report of the American College of Cardiology/American Heart Association Task Force on Practice Guidelines (Writing committee to revise the 1998 guidelines for the management of patients with valvular heart disease). *Circulation*. 2006;114:e84–e231.
4. Messika-Zeitoun D, Serfaty JM, Laissy JP, et al. Assessment of the mitral valve area in patients with mitral stenosis by multislice computed tomography. *J Am Coll Cardiol*. 2006;48: 411–413.
5. Rozenshtein A, Boxt LM. Computed tomography and magnetic resonance imaging of patients with valvular heart disease. *J Thorac Imaging*. 2000;15:252–264.
6. Otto CM, Bonow RO. Valvular heart disease. In: Libby P, Bonow RO, Mann DL, et al, eds. *Braunwald's Heart Disease*. 8th ed. Philadelphia, PA: Saunders Elsevier; 2008: 1625–1712.
7. Alkadhi H, Wildermuth S, Bettex DA, et al. Mitral regurgitation: quantification with 16-detector row CT—initial experience. *Radiology*. 2006;238:454.
8. Yachimski P, Lilly LS. Valvular heart disease. In: Lilly LS, ed. *Pathophysiology of Heart Disease*. 3rd ed. Baltimore, MD: Lippincott Williams & Wilkins; 2003:185–236.
9. Boxt LM. CT of valvular disease. *Int J Cardiovasc Imaging*. 2005;21:105–113.
10. Abbara S, Pena AJ, Maurovich-Horvat P, et al. Feasibility and optimization of aortic valve planimetry with MDCT. *AJR Am J Roentgenol*. 2007;188:356–360.
11. Alkadhi H, Wildermuth S, Plass A, et al. Aortic stenosis: comparative evaluation of 16-detector row CT and echocardiography. *Radiology*. 2006;240:47–55.
12. Bouvier E, Logeart D, Sablayrolles JL, et al. Diagnosis of aortic valvular stenosis by multislice cardiac computed tomography. *Eur Heart J*. 2006;27:3033.
13. Feuchtner GM, Dichtl W, Friedrich GJ, et al. Multislice computed tomography for detection of patients with aortic valve stenosis and quantification of severity. *J Am Coll Cardiol*. 2006;47:1410–1417.

14. Braverman AC, Guven H, Beardslee MA, et al. The bicuspid aortic valve. *Curr Probl Cardiol*. 2005;30:470–522.
15. Jacobs JE, Srichai M, Kim D, et al. Quadricuspid aortic valve: imaging findings on multidetector helical CT with echocardiographic correlation. *J Comput Assist Tomogr*. 2006;30:569–571.
16. Alkadhi H, Desbiolles L, Husmann L, et al. Aortic regurgitation: assessment with 64-section CT. *Radiology*. 2007;24:111–121.
17. Andrus BW, Baldwin JC. Infective endocarditis. In: Andrus BW, Baldwin JC, eds *Valvular Heart Disease*. London, UK: Manson Publishing Ltd; 2006:127–135.
18. Gilkeson RC, Markowitz AH, Balgude A, et al. MDCT evaluation of aortic valvular disease. *AJR Am J Roentgenol*. 2006;186:350–360.
19. Gowda RM, Khan IA, Nair CK, et al. Cardiac papillary fibroelastoma: a comprehensive analysis of 725 cases. *Am Heart J*. 2003;146:404–410.
20. Araoz PA, Mulvagh SL, Tazelaar HD, et al. CT and MR imaging of benign primary cardiac neoplasms with echocardiographic correlation. *Radiographics*. 2000;20:1303–1319.
21. Jones CB, Draughn T, Nomeir AM. Aortic valve thrombus presenting as a non-ST elevation myocardial infarction. *J Am Soc Echocardiogr*. 2008;21:876e1–876e3.
22. Daniel WG, Mügge A, Grote J, et al. Comparison of transthoracic and transesophageal echocardiography for detection of abnormalities of prosthetic and bioprosthetic valves in the mitral and aortic positions. *Am J Cardiol*. 1993;71:210–215.
23. Vogel-Claussen J, Pannu H, Spevak PJ, et al. Cardiac valve assessment with MR imaging and 64-section multi-detector row CT. *Radiographics*. 2006;26:1769–1784.
24. Kim RJ, Weinsaft JW, Callister TQ, et al. Evaluation of prosthetic valve endocarditis by 64-row multidetector computed tomography. *Int J Cardiol*. 2007;120:e27–e29.